OMEx-Diesel blends as high reactivity fuel for ultra-low NOx and soot emissions in the dual-mode dual-fuel combustion strategy

Antonio García*, Antonio Gil, Javier Monsalve-Serrano and Rafael Lago Sari

CMT - Motores Térmicos, Universitat Politècnica de València, Camino de Vera s/n, 46022 Valencia, Spain

Fuel, Volume 275, 1 September 2020, 117898
https://doi.org/10.1016/j.fuel.2020.117898

Corresponding author (*):
Dr. Antonio García Martínez (angarma8@mot.upv.es)
Phone: +34 963876574
Fax: +34 963876574

Abstract

Previous works demonstrated that the use of Oxymethylene ether (OMEx) in advanced combustion modes, as the dual-mode dual-fuel combustion, leads to a notable reduction of the lifecycle CO_2 emissions while promoting lower NOx and soot emissions than those from conventional diesel combustion. Nonetheless, the low heating value of OMEx results in a fuel consumption increase. A possible solution to avoid this drawback is by blending OMEx with diesel fuel. This will help to introduce the OMEx in the market with minimum changes in the infrastructure. In this context, this work evaluates the impact of using OMEx-diesel blends in different mass percentages (50% and 70% of OMEx in diesel), compared to the reference net fuels (net diesel and OMEx) in a multi-cylinder compression ignition engine operating under dual-mode dual-fuel combustion at different engine loads (25%, 50%, 80% and 100%) and 1800 rpm. At each condition, an air mass sweep was performed to assess the limiting operating conditions with each fuel due to either excessive pressure gradients and soot production, or low combustion efficiency. The results suggested that the OMEx-diesel blends allow to reduce the soot emissions compared to net diesel for all the conditions tested. In addition, blends having an OMEx mass content greater than 70% allowed to fulfill the EUVI limits for NOx with ultra-low soot levels (<0.01 g/kWh) up to 80% engine load. Nonetheless, the unique fuel able to achieve the EUVI limit for NOx with zero soot emissions simultaneously at 100% of engine load was found to be the pure OMEx.

Keywords

Dual fuel combustion; OMEx; e-fuels, EUVI emissions; synthetic fuels

1. Introduction

Since the environmental agreement reached in the 21st edition of the conference of parties (COP 21) [1], the European union searches alternatives for reducing the carbon dioxide footprint of the most used energy paths, aiming to achieve a low carbon energy matrix [2]. Regarding the mobility and transportation sector, several midterm solutions are being discussed, as the powertrain hybridization [3][4][5] and the use of e-fuels as alternative to the current fossil fuels [6][7]. These synthetic fuels present a significant number of advantages as their life cycle CO_2 reduction and the several raw materials to be extracted from [8]. Among the different fuels, Oxymethylene ether (CH_3–O–(CH2–O) x-CH_3, being x in the range of 1–6) stands as a potential surrogate for conventional diesel. The most significant properties of this fuel are the high oxygen content and the non-direct carbon bonds in its molecule [9]. These properties inhibit the soot formation, since the oxygen contained in the own molecule helps to oxidize the fuel and the non-direct carbon bonds difficulties the agglomeration of carbons to form solid particles [10]. Moreover, the most common path to produce this fuel uses CO_2 and H_2 as reactants submitted to reduction, oxidation and condensation reactions [11][12]. Therefore, depending on the electricity source, the CO_2 footprint can be significantly reduced [13].

Nonetheless, the transport properties differ from the diesel ones, meaning an impact on the fuel injection system (FIS).

In parallel to developing new fuels, the improvement of the conventional combustion devices in terms of their global efficiency and emissions have been also pursued [14]. These improvements can be also extended to the aftertreatment systems, increasing the regeneration [15] and filtration effectiveness [16], and, thereby reducing the amount of fuel spent on the diesel particulate filter processes. The low temperature combustion (LTC) strategies demonstrated to be an effective way in reducing pollutants as NOx and soot while maintaining similar or higher efficiency than the conventional diesel combustion [17]. The LTC is characterized by early injection timings together with high dilution levels to achieve fully premixed conditions. This enables a multisite ignition by the compression stroke, producing a fast combustion process. Besides, the high inert concentration can inhibit the NOx formation mechanism by reducing the in-cylinder temperature [18]. One of the most successful LTC concept is the reactivity-controlled compression ignition (RCCI) [19]. This combustion mode has the advantage of using two different fuels to achieve a well-controlled combustion process of short duration and low heat transfer [20], together with low soot and NOx emissions [21]. The first fuel (low reactivity fuel-LRF) is generally port fuel injected to create a preconditioned mixture field during the compression stroke [22]. The second one (high reactivity fuel-HRF) is direct injected from the half part of the compression stroke to increase the reactivity of the mixture and to create a charge stratification to promote the combustion to evolve [23]. Therefore, the combustion start and its progress can be controlled by modifying the ratio between the LRF and HRF, and the injection timings of the HRF [24][25]. However, the use of fully premixed conditions increases the unburned hydrocarbons

(HC) and carbon monoxide (CO) emissions due to the wall extinction and the fuel that enters into the piston gaps during the compression stroke. Recent investigations demonstrated that specific developments should be made in the diesel oxidation catalyst technology to address the level of these pollutants from RCCI combustion [26][27]. Moreover, a limitation of the RCCI combustion are the excessive mechanical requirements as the engine load is increased [28]. This is because a high quantity of energy is released in a short period, increasing rapidly the in-cylinder pressure [29]. Specific strategies to extend the maximum achievable load were proposed in the literature [30][31]. The use of dual-fuel multi-mode combustion process was successfully proposed and evaluated, enabling to realize full load operation by means of switching from a fully premixed combustion to a dual-fuel diffusive strategy. The fundamentals of this combustion approach are described in detail in [32]. The suggested combustion strategy allows to obtain similar operating range than the original engine calibration while maintaining the NOx values under the normative constraints in the worldwide harmonized vehicle cycle (WHVC) driving cycle with ultra-low soot levels [33].

The use of e-fuels in advanced combustion concepts seems to be a natural path to achieve the future regulated emissions and CO_2 reduction targets. The use of OMEx in the dual-fuel concept enables to compensate the drawbacks associated to the low heating value of this fuel by splitting the total required energy with the PFI fuel. In addition, it enables to promote premixed conditions at low load with low emissions and high efficiency. Moreover, its high oxygen content enhances the soot oxidation. This allows to use higher exhaust gas recirculation (EGR) levels at high-to-full, where diffusive operation is promoted, to avoid excessive pressure gradients and to reduce the NOx levels without excessive soot emissions. Nonetheless, the complete replacement of diesel by OMEx would require a significant modification of the engine injection system as well as a scaling in the production plants of this fuel. Therefore, the use of OMEx-diesel blends can be a midterm solution while the development, production and distribution networks of this fuel are established.

Investigations about the use of OMEx-diesel blends as well as net OMEx in dual-fuel concepts are still scarce in the literature. Therefore, this work is aimed to evaluate the impact of using OMEx-diesel blends (50% and 70% OMEx m/m in diesel) as well as net OMEx on the performance and emissions of the dual-mode dual-fuel combustion concept. A multi-cylinder dual-fuel engine platform was run under different operating conditions representative of the WHVC driving cycle. For each operating condition, a reference point was calibrated by means of a dedicated methodology, after which air mass sweeps were performed to assess the limiting conditions in terms of soot production and mechanical limitations. This allows to explore the potential of each fuel in realizing the normative constraints as well as the impact of achieving these limits on the engine performance compared to the conventional diesel-gasoline dual-fuel operation.

2. Materials and methods

This section addresses the different devices, materials and methods used during the investigation. First, the engine and test cell facilities are presented followed by a detailed description of the testing methodology for each operating condition.

2.1. Engine characteristics

The research was carried out in a multi-cylinder six-cylinders, 8L engine with the main characteristics described in Table 1. A few modifications were done to enable the dual-fuel combustion in this platform. First, the compression ratio was decreased from 17.5:1

to 12.75:1 to avoid excessive pressure gradients at high load conditions. Moreover, the piston geometry was designed to enhance the combustion process according to a specific methodology presented in a previous work [34]. Finally, six port fuel injectors (PFI) were mounted with a dedicated controller to fumigate the low reactivity fuel in the intake manifold. More details will be presented in the following sections.

Table 1. Engine characteristics.

Engine Type	4 stroke, 4 valves, direct injection
Number of cylinders [-]	6
Displaced volume [cm^3]	7700
Stroke [mm]	135
Bore [mm]	110
Piston bowl geometry [-]	Bathtub
Compression ratio [-]	12.75:1
Rated power [kW]	235 @ 2100 rpm
Rated torque [Nm]	1200 @ 1050-1600 rpm

2.2. Test cell description

The test cell facility scheme is presented in Figure 1, where the main measurements devices can be visualized. As it can be seen, a LP EGR system was added to the stock engine configuration to realize the high level of charge dilution required to achieve a fully premixed combustion. Since the temperature drop in the EGR line leads to the formation condensates, additional water filters were used to remove it before entering into the compressor [36]. Each individual cylinder is equipped with a Kistler 6125C cylinder pressure transducer to allow the visualization of possible dispersions on the air, EGR and LRF quantities (cylinder-to-cylinder dispersions). The data was collected with a resolution of 0.2 crank angle degree (CAD) using an AVL 364 encoder. The main regulated emissions were measured by means of a five-gas Horiba MEXA-7100 DEGR analyzer (NOx, HC, CO and CO_2). An AVL 415S smoke meter was used to obtain the smoke emissions in filter smoke number (FSN) units [35].

The HRF and LRF were measured by two AVL 733 S balances, allowing to obtain the instantaneous fuel consumption. Moreover, the air mass flow was measured by an Elster RVG G100 sensor. The average pressure and temperature values were also monitored and acquired at different locations, as presented in Figure 1. The low frequency data was acquired by means of an AVL PUMA interface at an acquisition rate of 10 Hz. This interface was also responsible to control the engine speed while the engine torque was regulated by the user. By contrast, the high frequency signals were recorded by means of a NI PXIe 1071 board. This board was connected to an in-house controller system that, besides of recording the raw data, has the ability to process the pressure data in real time to perform a heat release analysis. This allows to monitor the main combustion metrics as well as the HRR profile. The same NI board was also responsible for controlling the low reactivity and high reactivity fuel injection systems, except for the HRF injection pressure, and to control external devices as the back-pressure valve and the low pressure EGR quantity. Table 2 presents the accuracy of the main elements of the test cell.

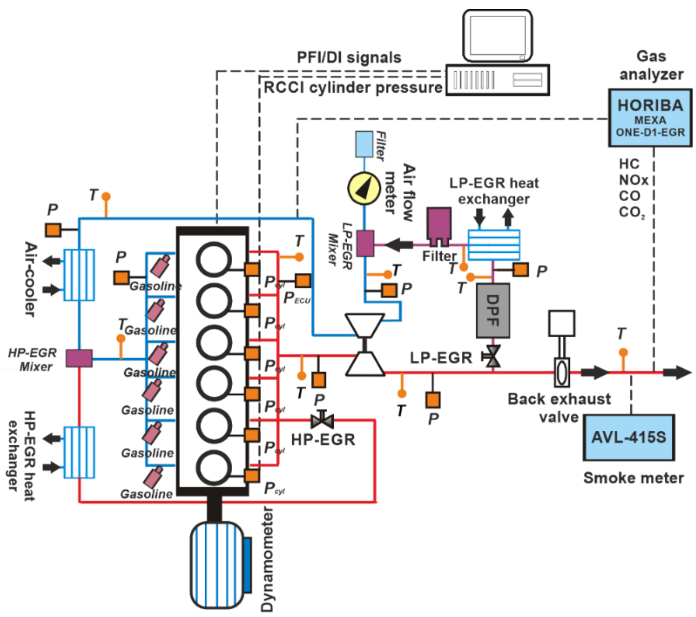

Figure 1. Test cell scheme.

Table 2. Accuracy of the instrumentation used in this work.

Variable measured	Device	Manufacturer / model	Accuracy
In-cylinder pressure	Piezoelectric transducer	Kistler / 6125C	±1.25 bar
Intake/exhaust pressure	Piezoresistive transducers	Kistler / 4045A	±25 mbar
Temperature in settling chambers and manifolds	Thermocouple	TC direct / type K	±2.5 °C
Crank angle, engine speed	Encoder	AVL / 364	±0.02 CAD
NOx, CO, HC, O_2, CO_2	Gas analyzer	HORIBA / MEXA 7100 DEGR	4%
FSN	Smoke meter	AVL / 415	±0.025 FSN
Gasoline/diesel fuel mass flow	Fuel balances	AVL / 733S	±0.2%
Air mass flow	Air flow meter	Elster / RVG G100	±0.1%

2.3. Fuels and injection systems characteristics

The different characteristics of the fuels used in this research are presented in Table 3. It is interesting to note that OMEx and diesel have significant differences in terms of composition, cetane number, density, lower heating value (LHV), etc. To ensure that both fuels can be properly mixed independently on their amounts, a preliminary study was done.

Table 3. Physical and chemical properties of the fuels.

	EN 228 gasoline	EN 590 diesel	OMEx
Density [kg/m^3] (T= 15 °C)	720	842	1067
Viscosity [mm^2/s] (T= 40 °C)	0.545	2.929	1.18
Cetane number [-]	-	55.7	72.9
Carbon content [% m/m]	-	86.2	43.6
Hydrogen content [% m/m]	-	13.8	8.82
Oxygen content [% m/m]	-	0	47.1
RON [-]	95.6	-	-
MON [-]	85.7	-	-
Lower heating value [MJ/kg]	42.4	42.44	19.04

The LRF was injected by means of a PFI system at 5.5 bar. The LRF injection timing was set at 340 CAD bTDC considering the results from previous studies [24]. The HRF was injected with the stock injection system whenever the fuel (diesel, OMEx or OMEx-diesel blend). The main injection parameters (injection timing and fuel mass) for the LRF and

HRF was controlled by means of a Labview software. The characteristics of the LRF and HRF fuel injection systems are depicted in Table 4.

Table 4. Characteristics of the direct and port fuel injectors.

Direct injector		Port fuel injector	
Actuation Type [-]	Solenoid	Injector Style [-]	Saturated
Steady flow rate @ 100 bar [cm^3/min]	1300	Steady flow rate @ 3 bar [cm^3/min]	980
Included spray angle [°]	150	Included Spray Angle [°]	30
Number of holes [-]	7	Injection Strategy [-]	single
Hole diameter [µm]	177	Start of Injection [CAD ATDC]	340
Maximum injection pressure [bar]	2500	Maximum injection pressure [bar]	5.5

2.4. Calibration methodology description

A dedicated calibration methodology was proposed to optimize the fuel consumption while respecting some pre-defined constrains. The calibration procedure is divided into three different steps. The first step addresses the load achievement in dual-fuel conditions and its logical scheme is presented in Figure 2. At first, the engine is started at CDC conditions and the gasoline amount is gradually increased aiming to achieve the maximum premix energy ratio (PER) (this assumption is reevaluated at the end of each calibration loop). At medium-to-high loads, the amount of energy released in a short period of time can result in excessive pressure gradients as well as high in-cylinder pressures. In these cases, the first action is to try to delay the start of injection to shift the end of the injection after the top dead center (TDC). Nonetheless, if the PER values are high, the energy from the gasoline dominates the combustion process. Therefore, it is required to decrease the PER as well as to delay the HRF start of injection (SOI) to avoid mechanical problems. After that, the calibration actions aim to ensure a stable combustion with coefficient of variation of the indicated mean effective pressure (COV_{IMEP}) values lower than 4%. Once the load is achieved while satisfying all these constraints, the next step is initiated.

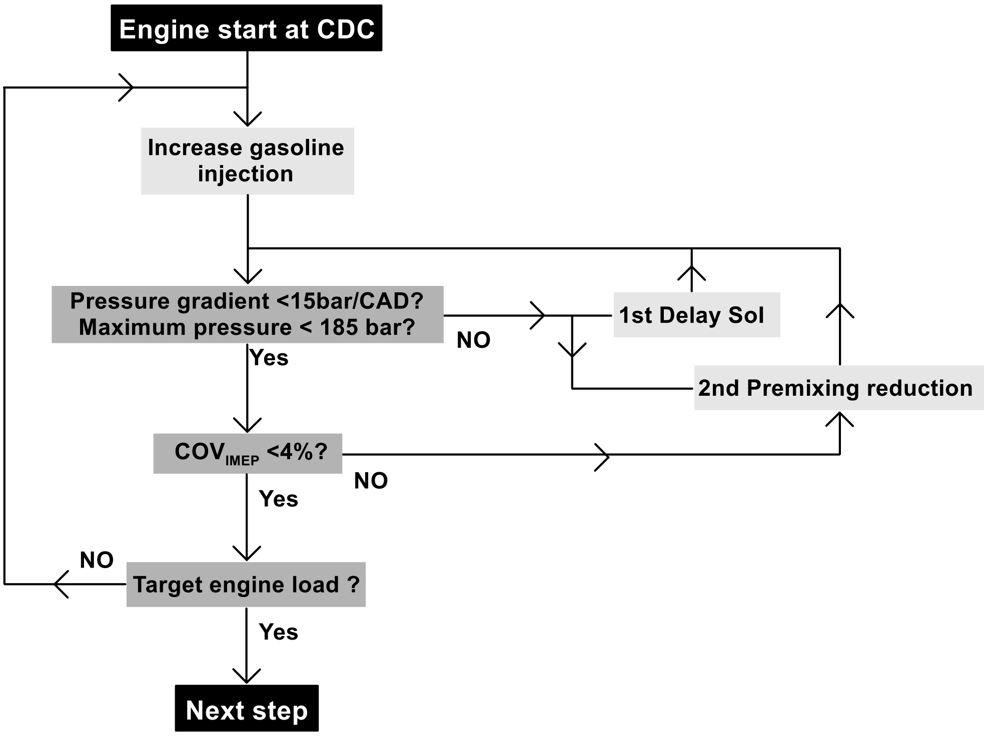

Figure 2. Representation of the different steps of the first stage of the calibration methodology.

Figure 3 depicts the second step of the calibration methodology. As it can be seen, it addresses the different scenarios that can be found for NOx and soot at the end of the first step: 1) NOx below the EUVI limit and soot below 0.01 g/kWh, 2) NOx above the EUVI limit and soot below 0.01 g/kWh, 3) NOx below the EUVI limit and soot above 0.01 g/kWh and 4) both pollutants above the limits. It should be remarked that a limit of 0.01 g/kWh has been imposed for soot, which corresponds to that imposed by the EURO VI regulation for PM emissions. Since soot measurements underestimate the gravimetric PM measurements with RCCI, this limit only ensures that tests with soot content above 0.01 g/kWh will be also out of EURO VI in terms of PM. However, for engine tests with soot levels below this limit, the compliance of EURO VI in terms of PM cannot be ensured, because their relationship depends on the engine operating conditions.

Different strategies are proposed to achieve the limits starting from the four scenarios described. In case of having higher NOx than EUVI, different strategies can be used. First, the EGR concentration can be increased to pursue higher dilution levels. In addition, the SoI can be delayed shifting the combustion towards the compression stroke, thus reducing the temperatures achieved during the combustion process. By contrast, if the soot levels are greater than 0.01 g/kWh, the in-cylinder mixture should be improved, and the oxygen concentration increased. The first can be achieved by improving the spray penetration, vaporization and mixing with higher injection pressure. In addition, earlier SOIs provide higher mixing times, reducing the zones with rich local equivalence ratios. Nonetheless, the most critical point to the soot oxidation is to provide enough oxygen to promote the soot oxidation reactions. This can be accomplished by both decreasing the EGR concentration as well as increasing the inlet pressure.

The most critical scenario after the first step of the calibration procedure is that in which both NOx and soot exceed the limits imposed. This is generally found at high load conditions, where part of the HRF is burned in a diffusive manner. Therefore, strategies to reduce both NOx and soot should be used. The first attempt to reduce the NOx emissions could be to increase the EGR concentration. Nonetheless, this would enhance the soot formation due to the decrease of the air fuel equivalence ratio. To counterbalance this, the turbine should be closed to increase the oxygen concentration at the intake and improve the soot oxidation. This last can be also reduced by means of early SOIs, increasing the fuel premixing and increasing the injection pressure. Generally, both strategies also have an impact on the NOx formation. In this sense, it is always tried to explore the hardware flexibility to achieve the emissions targets. However, in some cases, this cannot be accomplished, requiring to relax the constraints to achieve the desired engine load.

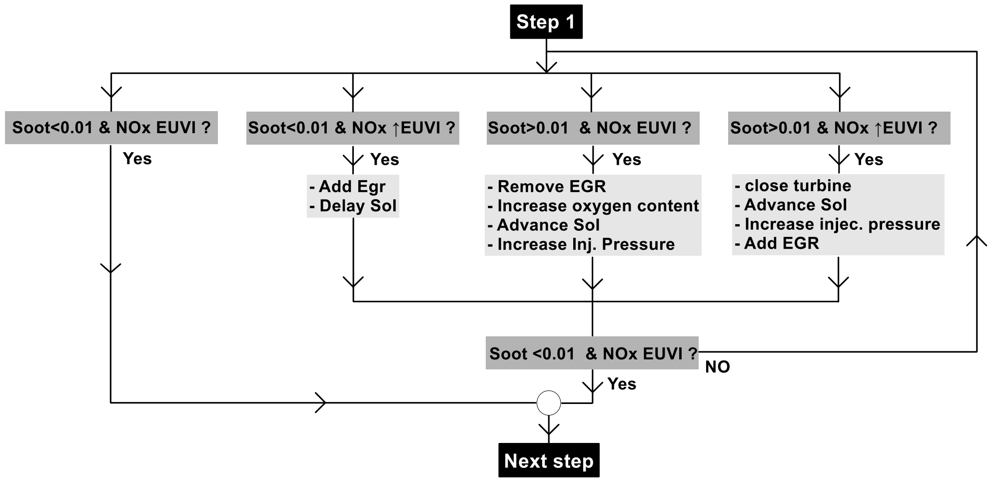

Figure 3. Representation of the different steps of the second stage of the calibration methodology.

The final step addresses the fuel consumption improvement by reducing the main losses during the conversion of the chemical into mechanical energy. The main sub-steps are presented in Figure 4. Each loop in the scheme represents the optimization of a specific loss. It should be noted that the optimization process is designed to continuing maintaining the constraints levels described in the previous step.

The first loop intends to decrease the pumping losses imposed to the engine by modifying the variable geometry turbine (VGT) position while providing the required EGR amount. In this sense, the proportion between LP and HP EGR as well as the VGT position are swept, aiming to provide the same amount of EGR and air while operating in a better efficiency at the turbine and with lower backpressure in the engine. The remaining loops aim to evaluate the effect of small modifications on the PER, SOI and EGR, trying to optimize the losses in combustion phasing and efficiency.

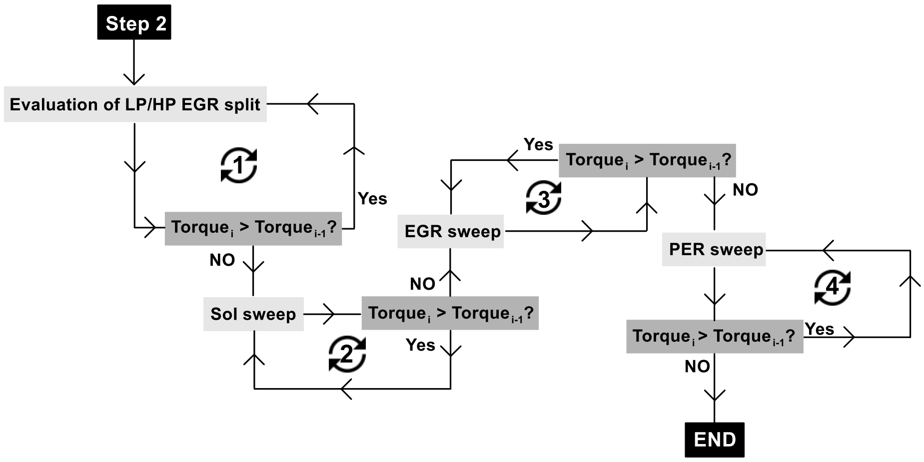

Figure 4. Representation of the different steps of the third stage of the calibration methodology.

A summary of the global calibration methodology and the main steps previously discussed are presented in Figure 5. It should be noted that at the end of the third step, a reevaluation of the PER value is done to ensure that the assumption of starting from the high PER is true and to avoid a local minimum as an optimum solution.

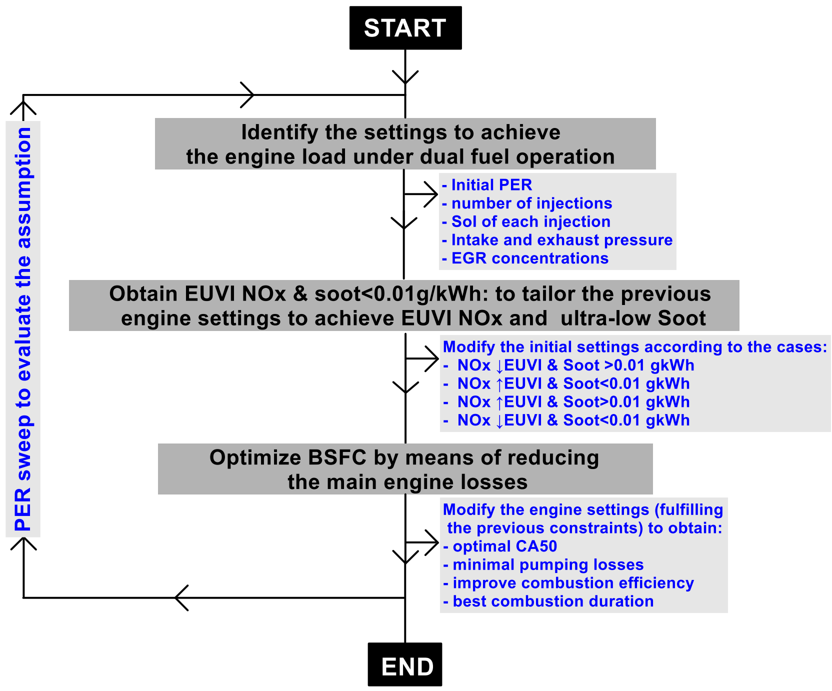

Figure 5. Summary of the methodology used to determine the reference condition for each fuel blend.

The results of fuel consumption are compared on an equivalent basis, i.e., considering the lower heating value of diesel as a reference. This was chosen as it excludes the impact of the lower heating value and allows to compare the fuel conversion efficiency of each blend and the pure OMEx to the diesel case. Equation 1 defines the equivalent brake specific fuel consumption ($BSFC_{eq}$) in terms of the mass of each fuel and the respective lower heating values.

$$BSFC_{eq}[g/kWh] = \frac{\dot{m}_{HRF} \cdot \left(\frac{LHV_{HRF}}{LHV_{diesel}}\right) + \dot{m}_{LRF} \cdot \left(\frac{LHV_{LRF}}{LHV_{gasoline}}\right)}{P_b} \quad (1)$$

3. Results and discussion

The results section is divided into four subsections corresponding to each engine load evaluated: 25%, 50%, 80% and 100%. For each one, the combustion, performance and emission results are discussed to illustrate the effect of the OMEx-diesel blends compared to the net fuels.

3.1. 25% of engine load

The first condition evaluated corresponds to the 25% of engine load. This operating condition is characterized by early HRF injections (≈ -30 CAD aTDC), promoting a highly premixed combustion. Moreover, the boundary and in-cylinder conditions allow to sweep the different EGR maps without problems of excessive pressure-gradients nor combustion inefficiency.

3.1.1. Combustion

Figure 6 presents the heat release profiles and pressure traces of the different HRF fuels evaluated for the reference condition obtained by means of the calibration methodology previously described. In addition, the injection rates for each fuel are presented in the top of the figure. The injection rates were obtained by means of an injection discharge rate curve indicator (IDRCI). More details about the measuring principle can be found in [37]. Therefore, the impact of the fuel modification in the injection system can also be evaluated for each reference condition. In this sense, it is possible to note that the use of net OMEx extends the injection rates to almost twice the duration of the diesel case, requiring to separate the injection dwell to avoid the injections to overlap. Mixtures containing diesel percentages equal or higher than 30% allowed to reduce the injection durations and use similar injection dwells than the reference diesel case. Table 5 presents the most relevant air management and injection settings obtained for each reference condition. It also allows to infer that the differences in the injection durations are directly impacted by the LRF fraction. This parameter quantifies the amount of mass injected by the port fuel systems with respect to the total mass (DI+PFI). In this sense, as the OMEx concentration is increased, the LRF fraction decreases as a consequence of its low LHV. It is interesting to note that the PER was maintained at similar levels for all the fuels.

Table 5. Air management and injection settings for the reference condition for each fuel evaluated at 25% of engine load.

	Diesel	50%OMEx	70%OMEx	OMEx
P_{intake} [bar]	1.4	1.4	1.4	1.4
T_{intake} [^oC]	53.1	54.9	55.8	55.5
M_{air} [g/s]	87.8	84.0	87.4	83.6
EGR [%]	41.3	43.1	41.6	43.7
SOI_{Pilot} [CAD bTDC]	32.0	32.0	32.0	33.0
SOI_{Main} [CAD bTDC]	18.0	18.0	18.0	17.0
PER [%]	42.0	44.3	45.1	44.3
LRF fraction [%]	42.2	37.1	33.9	26.2

The analysis of the heat release rate (HRR) profiles allows to conclude that this load is highly affected by the characteristics of the HRF. The first noticeable effect is the advance of the combustion start as the OMEx content is increased due to the higher cetane number of the mixture. This can be confirmed looking at the early combustion phases, which show an early low temperature heat release (LTHR) as the OMEx concentration is increased. This provides higher temperature in the combustion chamber, accelerating the reaction rates. In the end, the mixtures containing higher OMEx presented also and faster high temperature heat release rate.

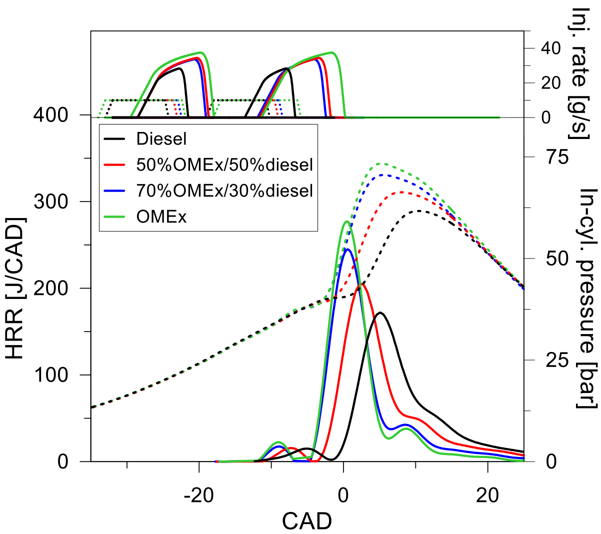

Figure 6. Heat release profiles for diesel, OMEx and blends of 50% m/m and 70% m/m of OMEx in diesel at the operating condition of 1800 rpm and 25 % of engine load.

Starting from the reference condition, the EGR concentration was modified in both directions to realize the effect of this parameter for the different fuels. Figure 7 (a) presents the results of $BSFC_{eq}$ for the different fuels and EGR levels evaluated. It is interesting to remark that the results are plotted against the NOx emissions, allowing to visualize the respective trade-offs with this contaminant. As previously discussed, the different NOx levels were obtained by sweeping the EGR by means of pre-stablished air mass variations (+10%, +5%, 0%, -5%, -10%) as always as possible.

At this engine load, low differences can be verified in terms of $BSFC_{eq}$ independently on the fuel. The highest differences are experienced at both limits, where higher dilution increases the fuel consumption and higher air mass allows to extend the net diesel operation to higher NOx values and lower fuel consumption. The most significant change can be seen in the case of OMEx, where almost all the conditions are inside the EUVI limits for NOx with lower $BSFC_{eq}$ values than the remaining fuels. This can be correlated to the faster combustion process, as depicted in Figure 8 (b), which results in lower residence time on high temperature zones, inhibiting the NOx formation. It is also possible to see that the combustion process tends to be faster as the OMEx concentration is increased. Figure 7 (b) presents the results of pressure gradient for the different fuels evaluated. Since the OMEx combustion occurs near the TDC and with a short duration, a high quantity of energy is release in a small volume. Consequently, the in-cylinder rises in a higher rate than the other cases. It is also interesting to note that a plateau is reached as the air mass is increased. From this point, the pressure gradient is not impacted, while the NOx emissions increase proportionally.

The combustion phasing (CA50) (Figure 8 (a)) and the combustion duration (Figure 8 (b)) present a similar trend, where the values are scaled according to the OMEx concentration. As the figure shows, the reactions start earlier and take place faster for the fuels with higher OMEx content, since they have a higher reactivity for the same premix energy ratio (PER). This behavior seems to be highlighted for lower EGR rates, where the exponential dependence of the activation energies increases the reaction rates.

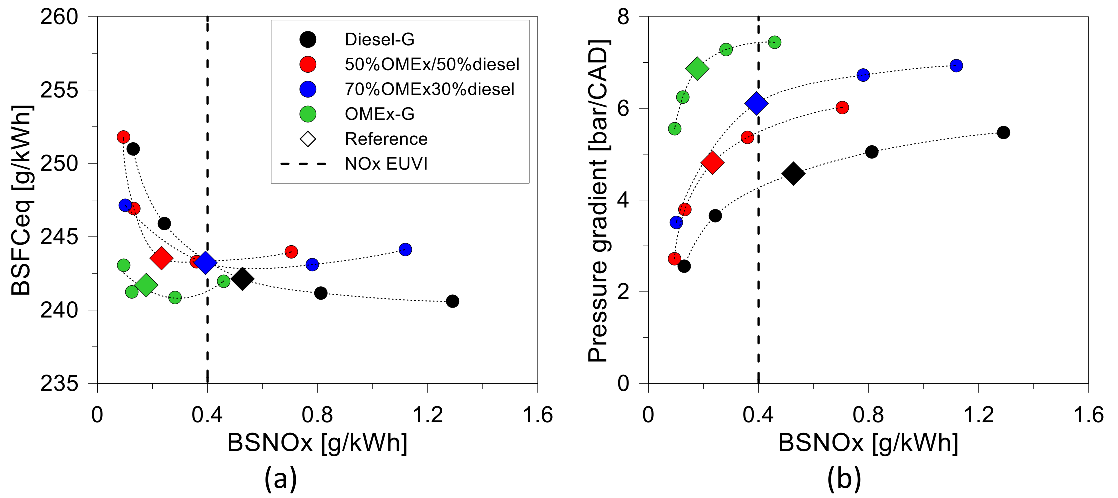

Figure 7. (a) Equivalent brake specific fuel consumption and (b) pressure gradient versus the engine-out NOx emissions for the different fuels at 1800 rpm and 25 % of engine load. The air mass is varied in steps of 5% around the reference condition.

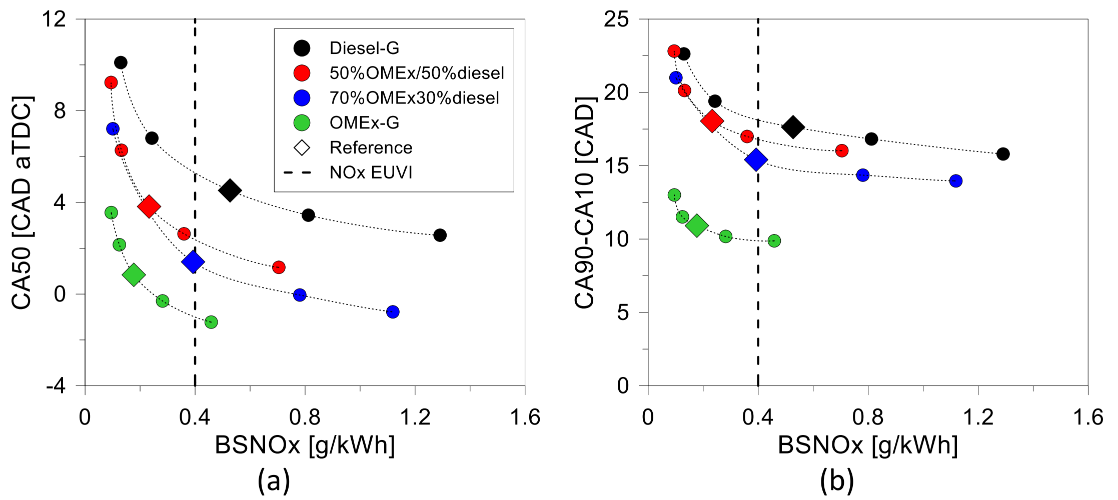

Figure 8. (a) Combustion phasing and (b) combustion duration versus the engine-out NOx emissions for the different fuels at 1800 rpm and 25 % of engine load. The air mass is varied in steps of 5% around the reference condition.

3.1.2. Emissions

The main regulated emissions for the 25% engine load condition are presented in Figure 9 and Figure 10. Figure 9(a) and Figure 9(b) show that HC and CO are positively affected by the OMEx content increase, confirming that the combustion efficiency is improved by increasing the cetane number of the fuel. Moreover, the levels of both contaminants increased with the EGR rate increase since the inert gases absorbs heat and decreases the reaction rates of the oxidation reactions.

Finally, the results of the NOx-soot tradeoff shown in Figure 10 suggest that this low load condition can reach the normative limits for NOx emissions while providing ultra-low soot emissions independently on the fuel used. This can be attributed to the fully premixed combustion characteristics in terms of large mixing times and short combustion durations. Consequently, both NOx and soot are minimized.

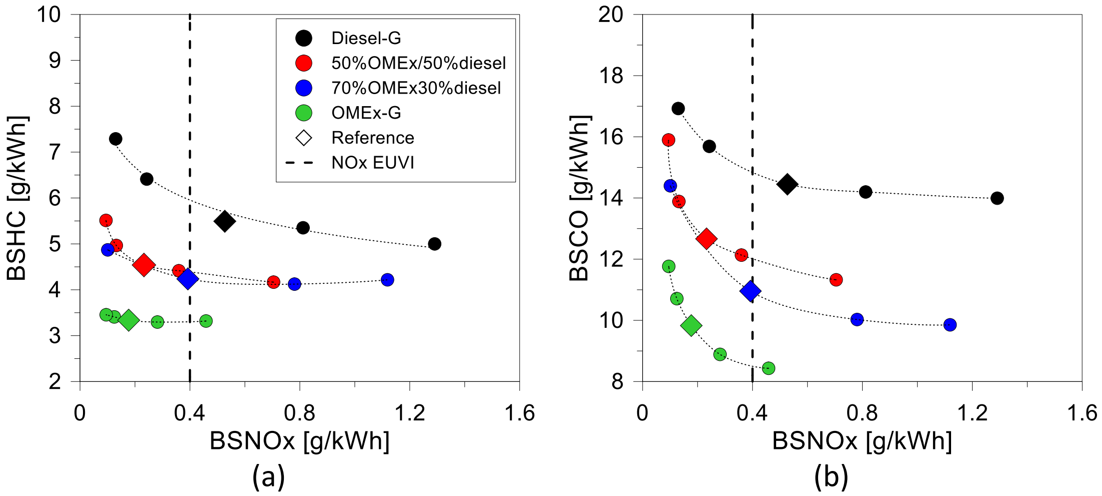

Figure 9. (a) Unburned hydrocarbon and (b) carbon monoxide emissions versus the engine-out NOx emissions for the different fuels at 1800 rpm and 25 % of engine load. The air mass is varied in steps of 5% around the reference condition.

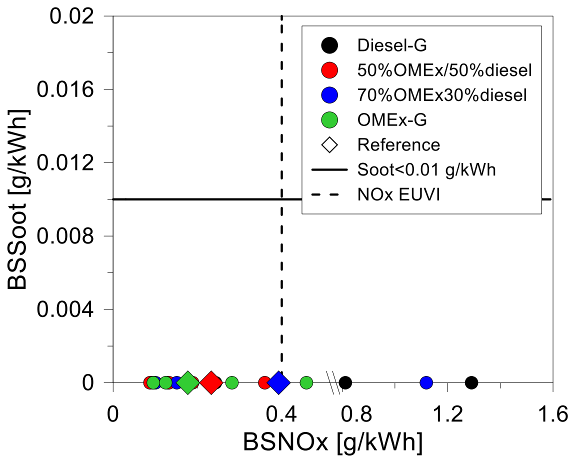

Figure 10. NOx-soot tradeoff for the different fuels at 1800 rpm and 25 % of engine load. The air mass is varied in steps of 5% around the reference condition.

3.2. 50% of engine load

The condition of 50% engine load presents higher PER values and earlier injection timings (-60 CAD aTDC) than the 25% engine load case, thus promoting a fully premixed combustion. In this way, NOx and soot can be inhibited simultaneously due to the fast combustion and large mixing times. Nonetheless, the influence of the HRF should be still significant as it will dictate the ignition delay of the mixture.

3.2.1. Combustion

Table 6 presents the injection and air management settings for the reference conditions at 50% engine load. It is possible to see that despite of using higher PER values than at 25% engine load, the heat release rates shown in Figure 11 seem to follow closely the trends presented in Figure 10. Again, the increase of the fuel reactivity due to the OMEx increase enhances the ignition process, resulting in early heat releases. Moreover, the high reactivity also results in a faster combustion process as the OMEx concentration is increased. It is interesting to note that the injection rates had to be increased to compensate the differences in the LHV and provide the same energy in the HRF.

Table 6. Air management and injection settings for the reference condition for each fuel evaluated at 50% of engine load.

	Diesel	50%OMEx	70%OMEx	OMEx
P_{intake} [bar]	2.1	2.0	2.1	2.0
T_{intake} [°C]	64.9	64.0	63.6	67.0
M_{air} [g/s]	122.5	122.9	122.6	118.4
EGR [%]	44.9	44.0	45.1	45.5
SoI_{Pilot} [CAD bTDC]	61.0	61.0	61.0	62.0
Soi_{Main} [CAD bTDC]	49.0	49.0	49.0	48.0
PER [%]	77.1	77.3	80.1	75.9
LRF fraction [%]	77.2	71.6	71.5	58.5

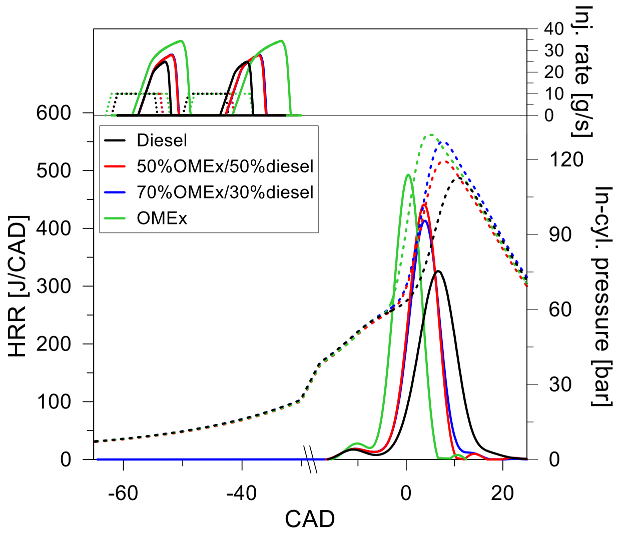

Figure 11. Heat release profiles for diesel, OMEx and blends of 50% m/m and 70% m/m of OMEx in diesel at the operating condition of 1800 rpm and 50 % of engine load.

Figure 12 (a) depicts the $BSFC_{eq}$ results for the different fuels and air levels. Most of the fuels present similar fuel consumption with respect to the NOx values, demonstrating that despite of having differences in the combustion process, it is possible to achieve similar efficiency at iso-NOx conditions. Nonetheless, it is possible to verify that the maximum NOx levels are consistently decreased as the OMEx content is increased. This fact suggests that the oxygen increase by the OMEx addition can result in leaner mixtures, decreasing the NOx concentration. In addition, the pressure gradients increase as the EGR is decreased, as presented in Figure 12 (b).

Additional information about the combustion process differences can be obtained by analyzing the combustion duration and combustion phasing values depicted in Figure 13. It seems that the fuel blends containing diesel, even in a low mass basis, still preserve the main combustion characteristics, presenting similar combustion duration and phasing, independently on the EGR levels. By contrast, the combustion process seems to be notably impacted when net OMEx is used, resulting in an earlier and faster combustion process. In fact, the step from 70% of OMEx to pure OMEx means a real increase of 60% on the OMEx mass. Considering that the cetane number is scaled directly with the fuel mass, this will result in a much more reactive mixture than the previous one, since the premixed energy (PER) ratio was maintained.

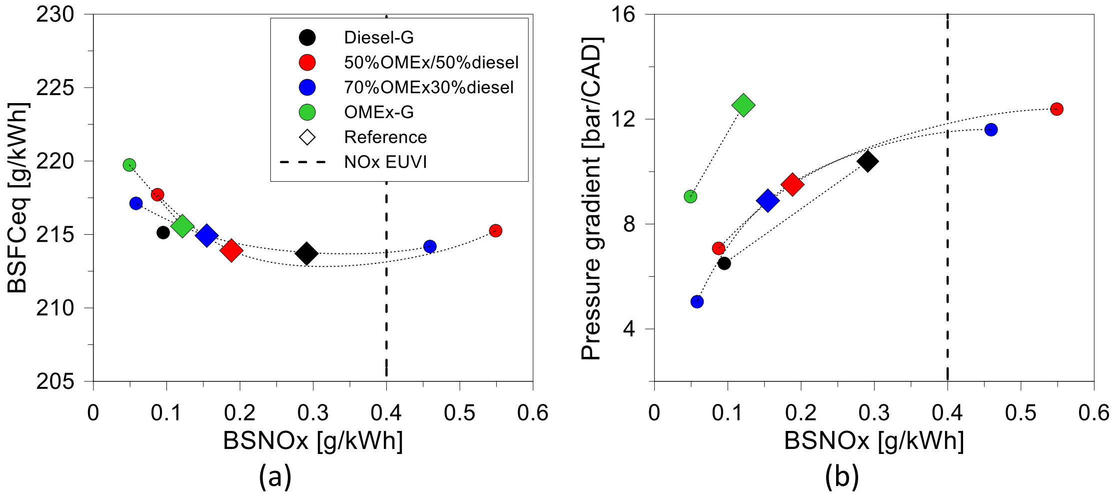

Figure 12. (a) Equivalent brake specific fuel consumption and (b) pressure gradient versus the engine-out NOx emissions for the different fuels at 1800rpm and 50 % of engine load. The air mass is varied in steps of 5% around the reference condition.

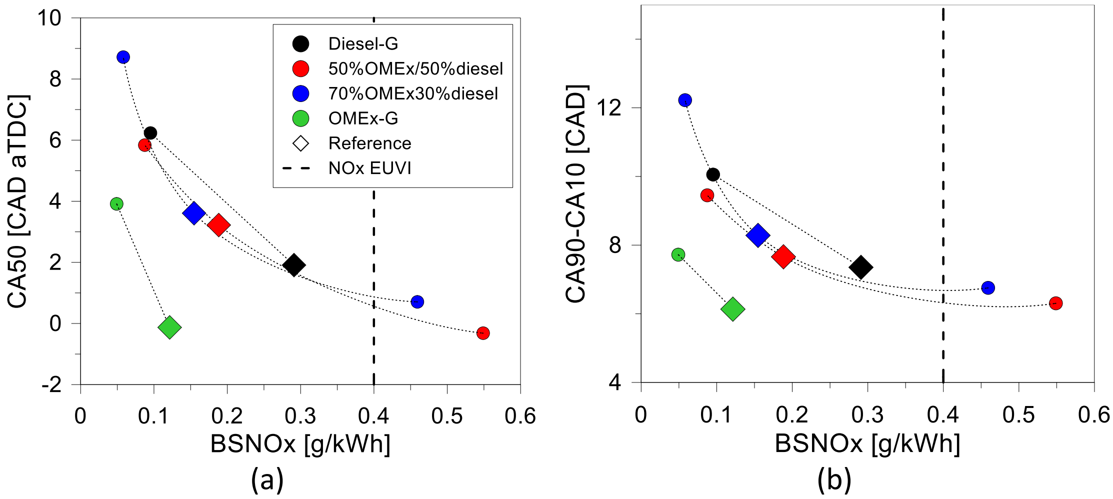

Figure 13. (a) Combustion phasing and (b) combustion duration versus the engine-out NOx emissions for the different fuels at 1800rpm and 50 % of engine load. The air mass is varied in steps of 5% around the reference condition.

3.2.2. Emissions

The impact of the different fuel compositions on CO and HC emissions are presented in Figure 14. The simultaneous analysis of both results allows to verify that CO and HC present a trade-off behavior, i.e., the cases with higher CO are those with lower HC. This allows to consider that the combustion efficiency is not highly impacted by the OMEx variation, which agrees with the results obtained from the equivalent fuel consumption. Moreover, the use of high EGR concentrations tends to increase exponentially the CO emissions. HC emissions are also negatively affected by the EGR increase, but in a less gradient than those of CO.

As previously discussed, the 50% engine load condition relies on a fully premixed combustion with high PER levels that should provide low levels of soot and NOx. This is confirmed in the results of Figure 15. As it can be seen, all the fuels are able to achieve normative constraints in terms NOx with a great margin and ultra-low soot emissions. Indeed, the NOx levels can be reduced to half of the normative, indicating that the concept can be able to realize future normative constraints.

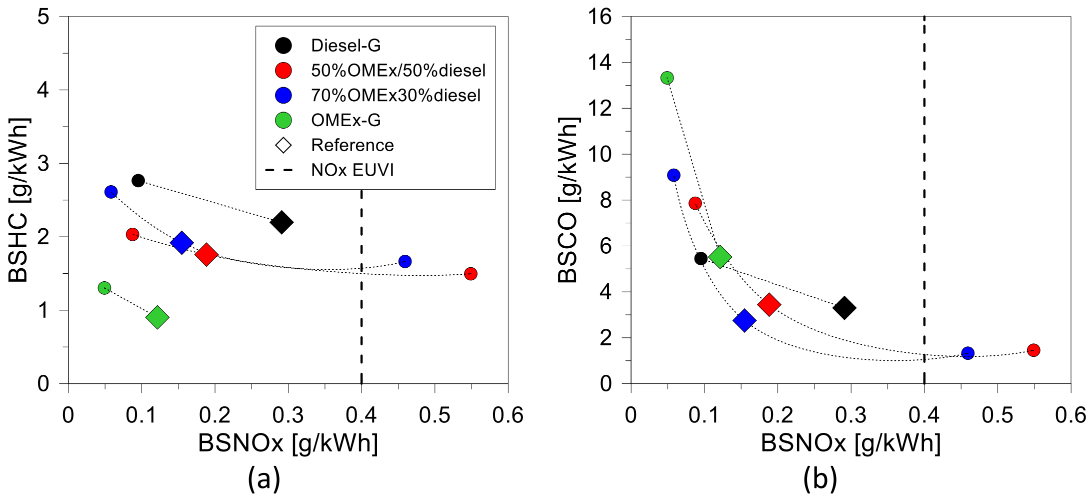

Figure 14. (a) Unburned carbon and (b) carbon monoxide emissions versus the engine-out NOx emissions for the different fuels at 1800rpm and 50 % of engine load. The air mass is varied in steps of 5% around the reference condition.

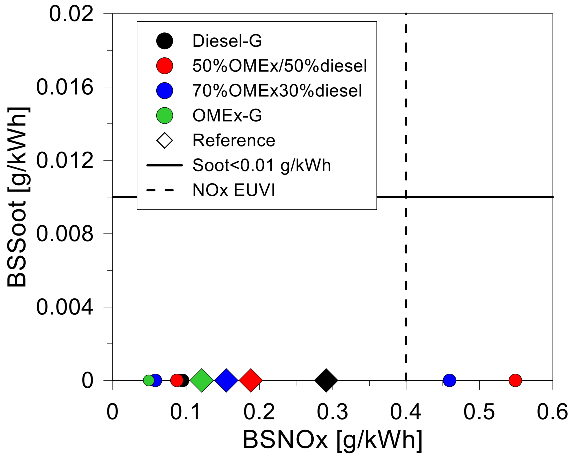

Figure 15. NOx-soot tradeoff for the different fuels at 1800rpm and 50 % of engine load. The air mass is varied in steps of 5% around the reference condition.

3.3. 80% of engine load

As the engine load is increased, the high energy released in a short period of time by the premixed combustion presents a challenge due to the consequent pressure gradients, which can exceed the mechanical constraints. In this sense, the operating strategy should be modified towards a more diffusive combustion relying on a single injection strategy for the HRF and on lower PER, as presented in Table 7. This enhances the soot production mechanism, requiring to relax the constraints of this pollutant to achieve NOx emissions levels under the normative constraint simultaneously.

3.3.1. Combustion

The heat release and pressure profiles as well as the injection rates for the different fuels at the reference condition are depicted in Figure 16. Their comparison provides insights about the combustion development along the cycle. It can be seen that the HRR profiles are similar, independently on the OMEx content in the fuel. This suggests that the modifications on the performance and emission parameters should be mainly attributed to the fuel properties and not to the combustion itself. Moreover, the different injection rates suggest that OMEx require almost two times higher mass than the conventional diesel. In addition, the injection rates seem to be scaled with the OMEx proportion in the blend. It is interesting to note that the pure OMEx injection lasts up to +20 CAD aTDC, increasing the total combustion duration.

Table 7. Air management and injection settings for the reference condition for each fuel evaluated at 80% of engine load.

	Diesel	50%OMEx	70%OMEx	OMEx
P_{intake} [bar]	2.8	2.8	2.8	2.8
T_{intake} [^{o}C]	57.5	57.3	52.6	53.7
M_{air} [g/s]	200.5	192.2	206.6	199.6
EGR [%]	34.6	36.5	36.6	36.0
SoI_{Pilot} [CAD bTDC]	-	-	-	-
Soi_{Main} [CAD bTDC]	8.0	8.0	8.0	8.0
PER [%]	53.2	56.0	52.5	55.6
LRF fraction [%]	53.4	48.5	40.8	35.9

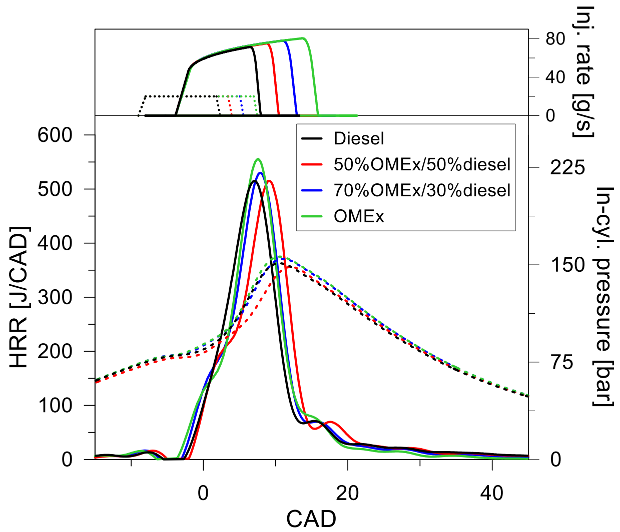

Figure 16. Heat release profiles for diesel, OMEx and blends of 50% m/m and 70% m/m of OMEx in diesel at the operating condition of 1800 rpm and 80 % of engine load.

The air sweep allows to explore the benefits of increasing the OMEx content on the blend. Net diesel operation is limited to just one operating condition (Figure 17 (a)). In this sense, the increase of air mass results in higher pressure gradients than the allowed limit, while the increase of EGR enhances the soot formation over the proposed limits. As the OMEx concentration is increased, the EGR sweep can be extended to more operating conditions, since the soot constraint is not surpassed. Thus, for the fuel blends having 50% of OMEx or more, three operating conditions can be achieved. The $BSFC_{eq}$

values shown in Figure 17 (a) suggests that the efficiency is not impacted by the fuel modification for the conditions with NOx levels higher than 0.2 g/kWh. Since the OMEx increase enhances the blend reactivity, the operation can be extended to higher dilution levels. Nonetheless, the combustion process starts to be delayed from the optimum point, resulting in a reduction of the final efficiency. This effect can be visualized in the CA50 results depicted in Figure 18 (a). The net OMEx and 70% OMEx allow to reach CA50 values higher than 10 CAD aTDC. It is clear that such delayed phasing should decrease the efficiency and increase the unburned products. Nonetheless, they offer a possibility to achieve NOx values over 4 times lower than the current normative. The increase of fuel consumption for higher EGR levels previously discussed can be also justified by the increase of the total combustion duration as presented in Figure 18 (b). This effect is widely addressed in the literature, being related to the reduction of the reaction rates by increasing the dilution levels [38].

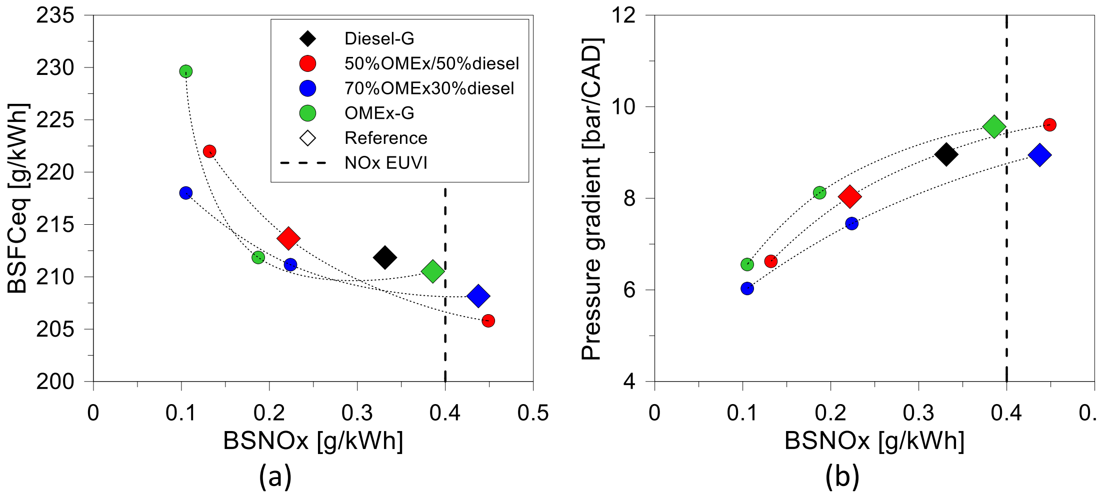

Figure 17. (a) Equivalent brake specific fuel consumption and (b) pressure gradient versus the engine-out NOx emissions for the different fuels at 1800 rpm and 80 % of engine load. The air mass is varied in steps of 5% around the reference condition.

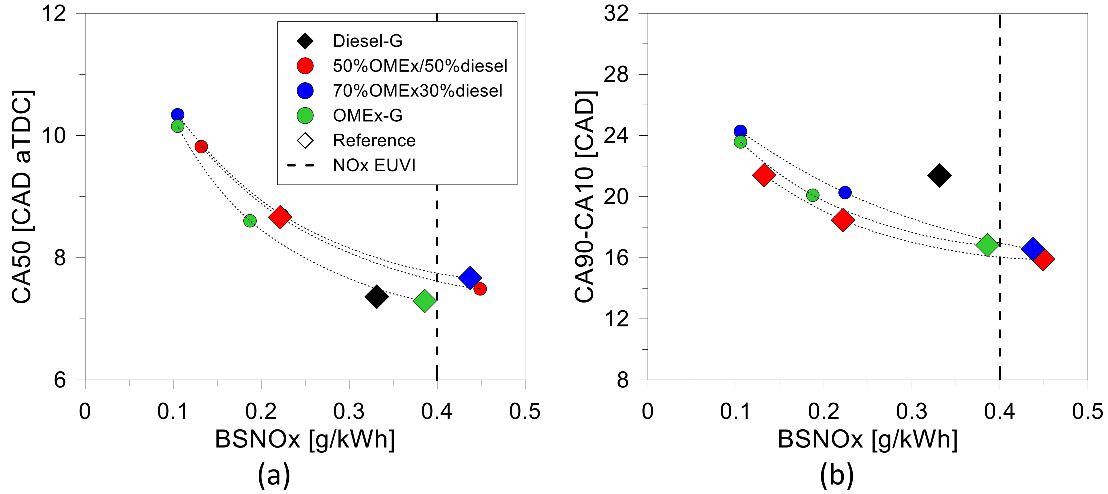

Figure 18. (a) Combustion phasing and (b) combustion duration versus the engine-out NOx emissions for the different fuels at 1800 rpm and 50 % of engine load. The air mass is varied in steps of 5% around the reference condition.

3.3.2. Emissions

The unburned HC as well as the CO emissions for the different operating conditions are depicted in Figure 19. Regarding the CO emissions (Figure 19 (a)), it is possibly to conclude that the emissions are scaled with the cetane number, i.e. the OMEx content, whose increase improves the global reactivity of the mixture and decreases the CO emissions. By contrast, the HC emissions are similar for the different air mass levels tested, independently on the fuel evaluated. This can be related to the amount of unburned HC that are formed near to the cylinder wall, as well as the fuel mass that remains into the piston crevices. As the gasoline mass is maintained for all the operating conditions and the HRF injection happens closer to the TDC, these near cylinder wall regions cannot be reached by the spray. In this sense, the LRF dominates the HC formation at this operating condition.

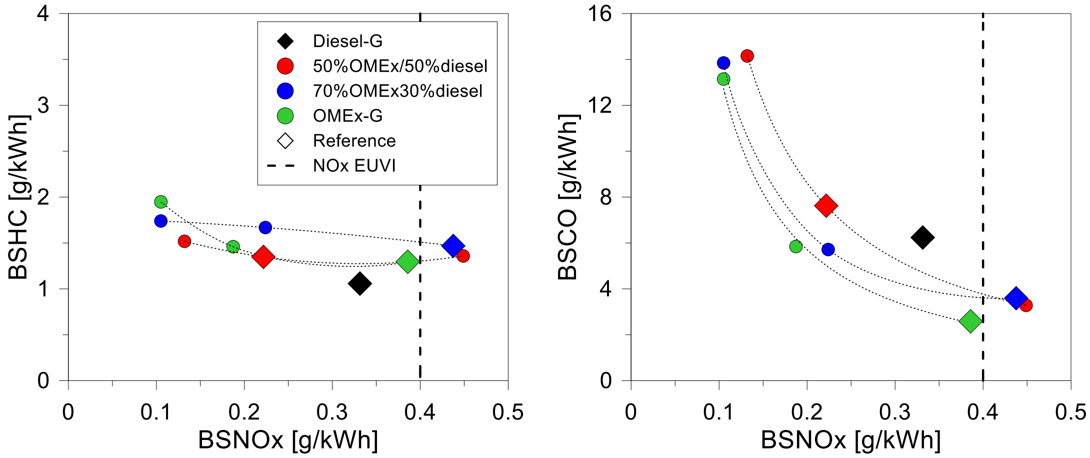

(a) (b)

Figure 19. (a) Unburned carbon and (b) carbon monoxide emissions versus the engine-out NOx emissions for the different fuels at 1800 rpm and 80 % of engine load. The air mass is varied in steps of 5% around the reference condition.

Figure 20 (a) presents the results for the soot-NOx tradeoff at 80% engine load. At this operating condition, the whole set of blends can achieve the EUVI limits in terms of NOx emissions. Nonetheless, the net diesel and blends with 50% of OMEx does not allow to achieve the soot target imposed. In the case of net diesel, the engine operation is limited to a unique point, since the decrease of the EGR amount results in excessive pressure gradients and the opposite action leads to exceed the soot limit by far. In the case of the 50% blend, the EGR levels can be modified. Nonetheless, the increase of the charge dilution increases the soot emissions whilst the decrease favors high temperatures, enhancing the NOx formation by the Zeldovich path. Therefore, this fuel blend never fulfills both constraints at the same time.

The increase of the OMEx content in the blend to 70% seems to be effective in reducing the soot emissions while maintaining similar conditions for the combustion process. Indeed, this blend can fulfill the soot target with a NOx threshold of 0.23 g/kWh (almost half of the EUVI limit). Even so, the most significant result is achieved with net OMEx, where zero soot emissions are realized independently on the dilution level used. Thus, it can be concluded that this fuel blend allows to achieve extremely low NOx levels with no soot emissions while maintaining its conversion efficiency. The mechanisms behind this effective reduction are still not fully addressed in the literature. As previously stated, recent works suggests that the oxygen concentration and the molecular structure of the fuel have significant impact on the soot path formation. Nonetheless, the importance of each mechanism is still not clear and future works are required to understand this phenomenon.

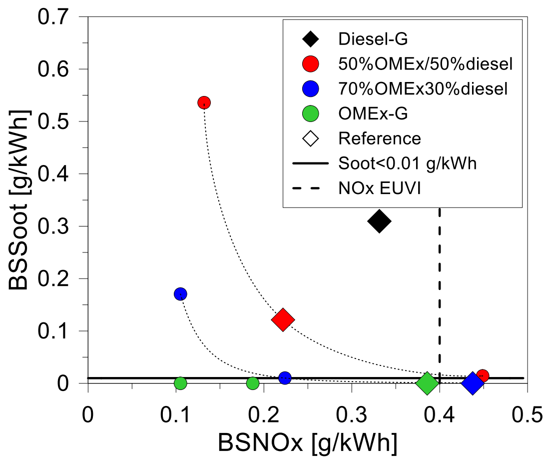

Figure 20. (a) NOx-soot tradeoff for the different fuels evaluated at 1800 rpm and 80 % of engine load. The air mass is varied in steps of 5% around the reference condition.

3.4. 100% of engine load

At full load operation, the critical conditions found at 80% engine load are magnified. This is because the fuel requirements as well as the in-cylinder temperature and pressure are higher than at the previous condition. Therefore, the combustion mode must be based on low premixing levels and low PER by prolonging the injection durations of the HRF. The main engine settings at high load are presented in Table 8.

3.4.1. Combustion

A similar analysis than that presented for the previous operating conditions can be done for the different HRR and in-cylinder pressure profiles presented in Figure 21 (a). First, the injection rates and the energizing times can be compared to assess the impact of the OMEx addition on the injection demand. Assuming that the diesel injector works on the flat region profile, the increase of the energizing time could be directly related to the time that the injector remains fully opened. This can be visualized in the injection rate profiles of Figure 21 (a). The calculation of the percentage difference among them results in an increase of 18 %, 28.5% and 42% in the energizing time to compensate the LHV differences of 27.6%, 38.6% and 55.2% compared to the net diesel case. The ratio between the percentages for each fuel provides values of 1.53, 1.36 and 1.3, demonstrating that, as the OMEx concentration is increased, more mass is injected in the same period. This can be justified by the higher density of the OMEx compared to the commercial diesel as previously depicted in Table 3.

Table 8. Air management and injection settings for the reference condition for each fuel evaluated at 100% of engine load.

	Diesel	50%OMEx	70%OMEx	OMEx
P_{intake} [bar]	2.9	2.9	2.8	2.9
T_{intake} [^{o}C]	53.4	52.3	51.5	53.5
M_{air} [g/s]	252.4	251.6	248.0	249.2
EGR [%]	22.1	20.9	22.1	24.2
SoI $_{Pilot}$ [CAD bTDC]	-	-	-	-
Soi $_{Main}$ [CAD bTDC]	7.0	7.0	7.0	7.0
PER [%]	32.9	32.6	34.3	33.5
LRF fraction [%]	33.0	26.4	24.6	18.4

The effect of increasing the injection duration can be noted at the HRR profiles. It is suggested that two different mechanisms are impacting the development of the combustion process. First, the premixed gasoline experiences a fast burning process, releasing high amounts of energy closer to the TDC. Once the gasoline is burned, the HRF supports the combustion process to achieve the desired engine load. This assumption is based on the analysis of Figure 21 (b). If one moves the HRR trace from pure OMEx to match it with the others, it is possible to see that all the fuel blends presents a similar peak on the HRR profile. Considering that the gasoline remains constant for all the cases, i.e., same PER, it should be perceived modifications on the HRR in the case of burning high amounts of HRF. Nonetheless, the HRR does not present significant modifications neither in its shape nor in the absolute values for the premixed phase. From the 8 CAD ATDC, the HRR profiles starts to decouple, suggesting that from these conditions, the HRF starts to dominate the energy release by means of a diffusive combustion. The last combustion phase allows to visualize the effects of the low LHV of the blends with higher OMEx content, which is considerably extended as the OMEx is increased.

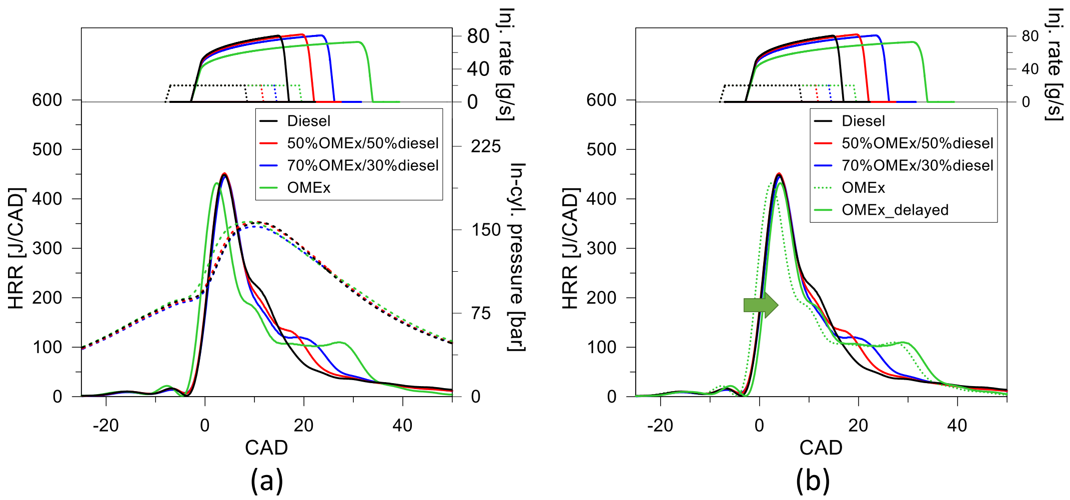

Figure 21. (a) Heat release profiles for diesel, OMEx and blends of 50% m/m and 70% m/m of OMEx in diesel at the operating condition of 1800 rpm and 100 % of engine load and (b) comparison of the heat release rates with shift OMEx combustion.

The use of low PER values leads to a large diffusive part of the combustion process. Therefore, it is expected that the losses due to excessive combustion durations would be amplified as the OMEx content is increased. This fact is confirmed by the $BSFC_{eq}$ results depicted in Figure 22 (a). Considering the NOx values of the diesel-gasoline reference and extending the trend lines to this point, it is possible to see that the use of blends containing up to 70% of OMEx does not reduce significantly the engine efficiency. Nevertheless, the pure OMEx case requires a significant increase in the time to be burned, increasing the final $BSFC_{eq}$. It is also interesting to note that all the mixtures reached a similar threshold of pressure gradient without surpassing the limit of 10 bar/CAD. This means that the previous statement of the low participation of OMEx in the combustion should be corrected in the case of net OMEx. For this condition, the combustion is considerably accelerated, meaning a steeply increase in the HRR and consequently on the pressure gradients.

The critical conditions verified at 80% of engine load are amplified at full load operation, since more fuel is required and the temperature and pressure inside the cylinder are higher. Therefore, the combustion mode should be based on low premixing levels, with even more reduced PER compared to the previous condition.

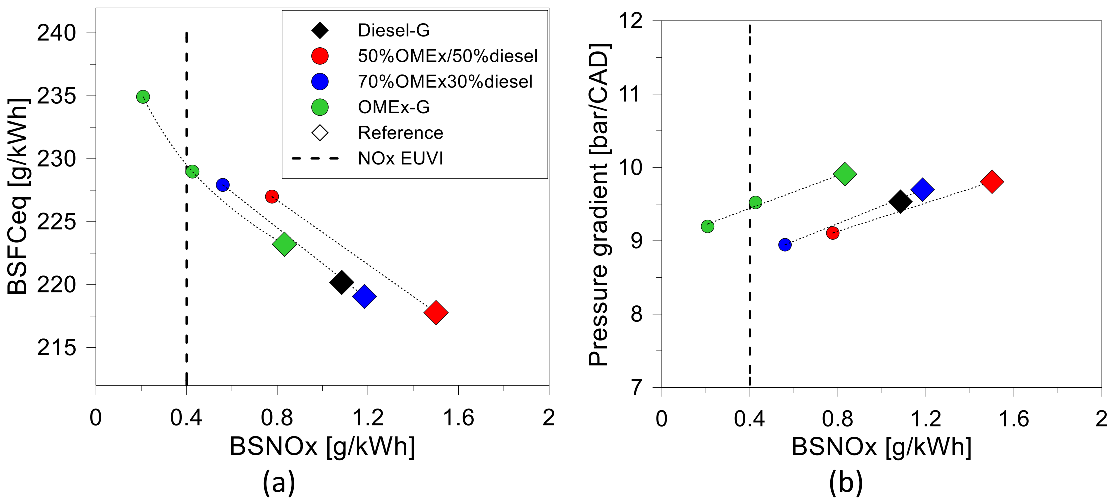

Figure 22. (a) Equivalent brake specific fuel consumption and (b) pressure gradient versus the engine-out NOx emissions for the different fuels at 1800 rpm and 100 % of engine load. The air mass is varied in steps of 5% around the reference condition.

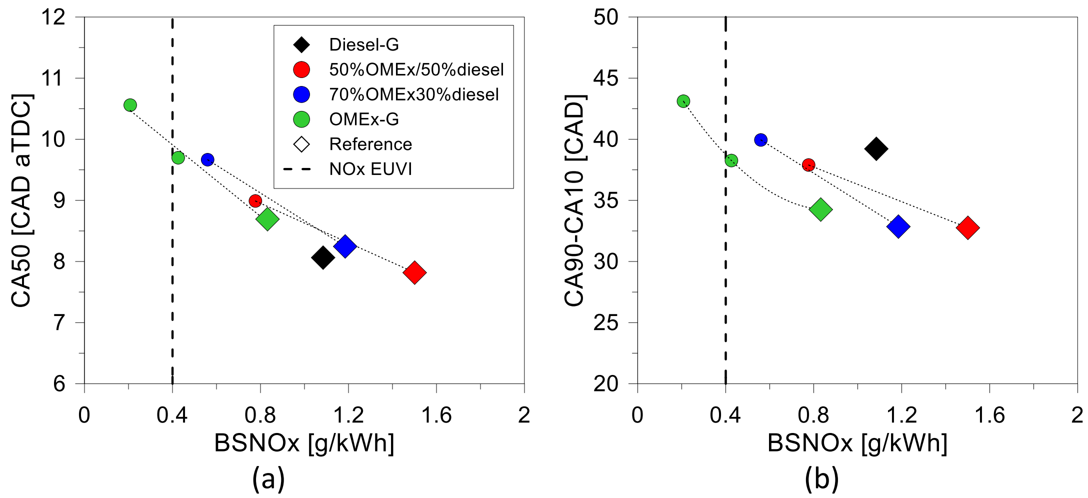

Figure 23. (a) Combustion phasing and (b) combustion duration versus the engine-out NOx emissions for the different fuels at 1800 rpm and 100 % of engine load. The air mass is varied in steps of 5% around the reference condition.

3.4.2. Emissions

Figure 24 and Figure 25 show the emissions results for the full load condition. Figure 24 (a) and Figure 24 (b) depict the HC and CO results for the different fuels. As it can be seen, the increase of the OMEx content allows to improve the CO-NOx trade-off. This can be explained by the higher reactivity of the fuel attributed to the OMEx cetane number and the leaner global mixtures promoted by the oxygen content in the fuel molecule. By contrast, the HC emissions present similar values for almost all the operating conditions, only increasing in the OMEx cases with dilution levels. Nonetheless, as consequence of the diffusive combustion process, the HC levels are lower compared to the conventional premixed strategies presented in previous sections.

Finally, the NOx-soot tradeoffs for the different fuels are presented in Figure 25 (a). From the figure, it can be seen that none of the fuel blends are able to fulfill the EUVI NOx limits and the self-imposed soot target (0.01 g/kWh) simultaneously. This is consequence of using low PER, which enhances the soot formation due to the diffusive combustion. Moreover, the large combustion process found at this condition also contributes to worsen the soot oxidation phenomenon. For the tests performed, it was found that pure OMEx was the unique fuel able to achieve the EUVI limits for NOx with ultra-low soot emissions simultaneously.

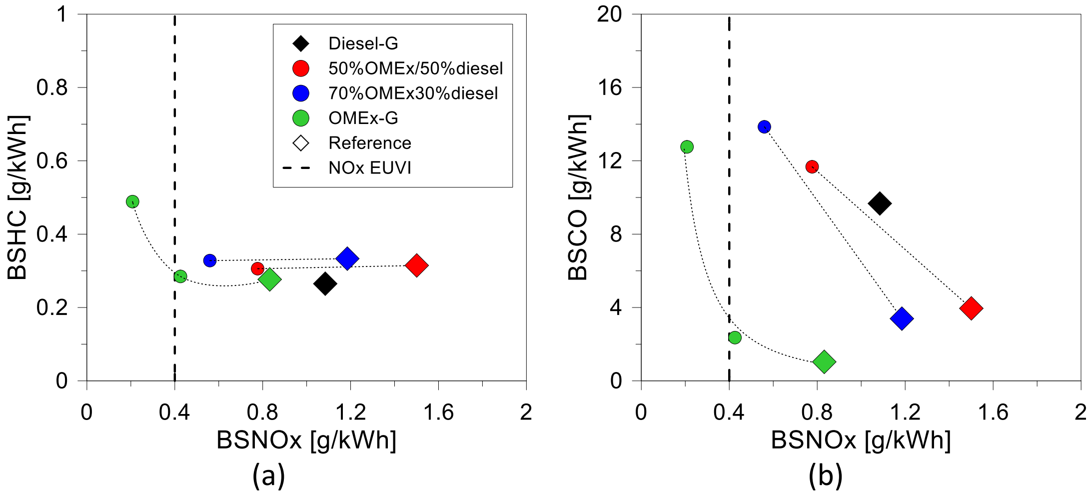

Figure 24. (a) Unburned carbon and (b) carbon monoxide emissions versus the engine-out NOx emissions for the different fuels at 1800rpm and 100% of engine load. The air mass is varied in steps of 5% around the reference condition.

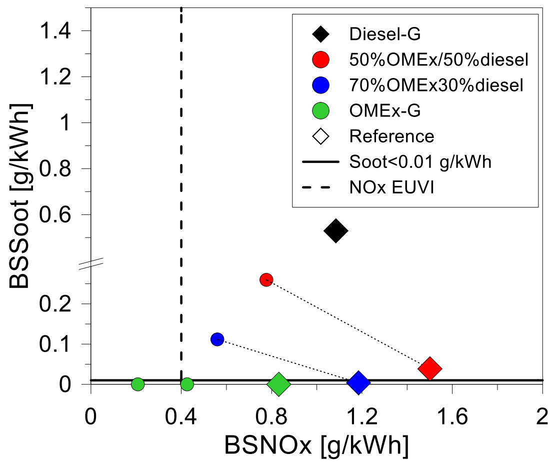

Figure 25. NOx-soot tradeoff for the different fuels evaluated at 1800rpm and 100 % of engine load. The air mass is varied in steps of 5% around the reference condition.

4. Conclusions

This work investigated the impact of using diesel-OMEx blends in a dual-mode dual-fuel engine at different engine loads representative of the WHVC conditions. For each engine load, an air mass sweep was performed by modifying the EGR levels to assess the limits of each fuel in terms of pressure gradient, soot production and combustion efficiency. This allowed to determine the potential of each fuel in terms of the minimum soot or minimum NOx achievable. It is possible to conclude that the use of OMEx has different effects on the dual-mode dual-fuel combustion according to the different combustion regimes found at different loads:

- Low-to-medium load (fully premixed combustion): in these conditions the PER values are high and the role of the HRF is to pre-condition the mixture and provide ignitable conditions. In this sense, the increase of the reactivity from the OMEx resulted in lower combustion durations and early combustion starts, perceived also in the LTHR. As these conditions, the dual-mode dual-fuel combustion does not produce soot and NOx whatever the fuel.
- High-to-full load (dual-fuel diffusive combustion): as the PER is decreased and the combustion regime is modified to a diffusive combustion, the HRF becomes dominant impacting the combustion start and providing the most of the energy needed to achieve the desired load. Therefore, the increase of the OMEx content in the blend allows to reduce both soot and NOx emissions, achieving NOx EUVI limits up to 80% of engine load with soot emissions lower than 0.01 g/kWh. By contrast, this previous scenario can be only achieved at full load with pure OMEx.

Based on this summary, it can be concluded that the use of OMEx-diesel blends in the dual-mode dual-fuel combustion can be a short-term solution for the transition to a low carbon transportation scenario. The use of mixtures with 70% of OMEx in diesel provided similar fuel consumption than the conventional diesel while achieving EUVI

NOx up to 80% of engine load with soot values lower than 0.01 g/kWh. In addition, the soot production at full load is significantly reduced with this fuel. Since the operating condition distribution along a driving cycle rarely achieves the full load operation, it is believed that the concept can reach the normative limits without the addition of after treatment system for NOx while delivering ultra-low soot emissions reducing both the customer and operational costs. It is interesting to note that the use of the different fuel ratios increases the demand over the fuel injection system due to the higher injection durations and high flows through the high-pressure pump, which can lead to the system failure.

Finally, it should be remarked that EUVI normative limits both particulate matter and particulate number. In this sense, dedicated studies should be performed to assess the effect of using OMEx on the particulate production on representative operating conditions. Moreover, the OMEx oxidation mechanism and the different paths that are responsible to deliver zero soot in the exhaust gases should be investigated.

Acknowledgments

The authors thanks ARAMCO Overseas Company and VOLVO Group Trucks Technology for supporting this research. The authors acknowledge FEDER and Spanish Ministerio de Economía y Competitividad for partially supporting this research through TRANCO project (TRA2017-87694-R). The authors also acknowledge the Universitat Politècnica de València for partially supporting this research through Convocatoria de ayudas a Primeros Proyectos de Investigación (SP20180148). The author R. Sari acknowledges the financial support from the Spanish ministry of science innovation and universities under the grant “Ayudas para contratos predoctorales para la formación de doctors” (PRE2018-085043).

References

[1] United Nation climate change: the paris agreemen. Available at <https://unfccc.int/process-and-meetings/the-paris-agreement/the-paris-agreement accessed in 05/02/2020>.

[2] Soler A. Role of e-fuels in the European transport system. Literature review. Concawe, Brussels, January 2020.

[3] Benajes J., García A., Monsalve-Serrano J., Martínez-Boggio S. Optimization of the parallel and mild hybrid vehicle platforms operating under conventional and advanced combustion modes. Energy Conversion and Management, Volume 190, 2019, Pages 73-90, ISSN 0196-8904.

[4] Luján J. M., García A., Monsalve-Serrano J., Martínez-Boggio S. Effectiveness of hybrid powertrains to reduce the fuel consumption and NOx emissions of a Euro 6d-temp diesel engine under real-life driving conditions, Energy Conversion and Management, Volume 199, 2019.

[5] Benajes, J., García, A., Monsalve-Serrano, J., Sari, R. Potential of RCCI series hybrid vehicle architecture to meet the future CO2 targets with low engine-out emissions Applied Sciences (Switzerland)8(9),2018,1472

[6] Pastor J. V., García A., Micó C., Lewiski F. An optical investigation of Fischer-Tropsch diesel and Oxymethylene dimethyl ether impact on combustion process for CI engines. Applied Energy, Volume 260, 2020, 114238, ISSN 0306-2619, https://doi.org/10.1016/j.apenergy.2019.114238.

[7] Ershov M., Potanin D., Gueseva A., Abdellatief T., Kapustin V. Novel strategy to develop the technology of high-octane alternative fuel based on low-octane gasoline Fischer-Tropsch process. Fuel, Volume 261, 2020.

[8] Verhelst, S., Turner, J.W.G., Sileghem, L., Vancoillie, J. Methanol as a fuel for internal combustion engines. Progress in Energy and combustion science. Volume 70, October 2019, pages 43-88.

[9] Deutz, S., Bongartz, D., Heuser, B., Kätelhön, A., Schulze, L.L., Omari, A., Walters, M., Klankermayer, J., Leitner, W., Mitsos, A., Pischinger, S., Bardow, A. Cleaner production of cleaner fuels: wind-to-wheel – environmental assessment of CO2-based oxymethylene ether as a drop-in fuel. Energy Environ. Science, November 2017, Volume 11, pages 331-343.

[10] Omari, A., Heuser, B., Pischinger, S. Potential of oxymethylenether-diesel blends for ultra-low emission engines, Fuel, Volume 209, 2017, pages 232-237, ISSN 0016-2361, https://doi.org/10.1016/j.fuel.2017.07.107.

[11] Burre, J., Bongartz, D., Mitsos, A. Production of Oxymethylene Dimethyl Ethers from Hydrogen and Carbon Dioxide—Part I: Modeling and Analysis for OME1. Industrial & Engineering Chemistry Research, March 2019, Volume 58, pages 4881-4889, DOI: 10.1021/acs.iecr.8b05576

[12] Burre, J., Bongartz, D., Mitsos, A. Production of Oxymethylene Dimethyl Ethers from Hydrogen and Carbon Dioxide—Part II: Modeling and Analysis for OME3–5 Industrial & Engineering Chemistry Research, March 2019, Volume 58, pages 5567-5578, DOI: 10.1021/acs.iecr.8b05577

[13] García A., Monsalve-Serrano J., Villalta D., Sari R., Zavaleta V, Gaillard P. Potential of e-Fischer Tropsch diesel and oxymethyl-ether (OMEx) as fuels for the dual-mode dual-fuel concept. Applied Energy, Volume 253, 2019, 113622.

[14] Payri, R., De La Morena, J., Monsalve-Serrano, J., Pesce, F.C., Vassallo, A. Impact of counter-bore nozzle on the combustion process and exhaust emissions for light-duty diesel engine application. International Journal of Engine Research 20(1), pp. 46-57,2019.

[15] Di Sarli V, Landi G, Lisi L, Saliva A, Di Benedetto A. Catalytic diesel particulate filters with highly dispersed ceria: Effect of the soot-catalyst contact on the regeneration performance. Applied Catalysis B: Environmental, Volume 197, 2016, Pages 116-124.

[16] Orihuela M. P, Gómez-Martín A, Miceli P, Becerra J, Chacartegui R, Fino D. Experimental measurement of the filtration efficiency and pressure drop of wall-flow diesel particulate filters (DPF) made of biomorphic Silicon Carbide using laboratory generated particles. Applied Thermal Engineering, Volume 131, 2018, Pages 41-53.

[17] Pachiannan T., Zhong W., Rajkumar S., He Z., Leng X., Wang Q. A literature review of fuel effects on performance and emission characteristics of low-temperature combustion strategies. Applied Energy, Volume 251,2019,113380.

[18] Martins, M., Fischer, I., Gusberti, F., Sari, R. et al., "HCCI of Wet Ethanol on a Dedicated Cylinder of a Diesel Engine," SAE Technical Paper 2017-01-0733, 2017, https://doi.org/10.4271/2017-01-0733.

[19] Reitz, R.D., Duraisamy, F. Review of high efficiency and clean reactivity-controlled compression ignition (RCCI) combustion in internal combustion engines. Progress in Energy and Combustion Science. Volume 46, August 2014, pages 12-71

[20] Olmeda P, García A, Monsalve-Serrano J, Sari R. Experimental investigation on RCCI heat transfer in a light-duty diesel engine with different fuels: Comparison versus conventional diesel combustion. Applied Thermal Engineering, Volume 144, November 2018, Pages 424-436.

[21] Benajes J., García A., Monsalve-Serrano J, Sari R. Fuel consumption and engine-out emissions estimations of a light-duty engine running in dual-mode RCCI/CDC with different fuels and driving cycles. Energy, Volume 157, 2018, Pages 19-30.

[22] Curran S, Hanson R, Wagner R. Reactivity controlled compression ignition combustion on a multi-cylinder light-duty diesel engine. International Journal of Engine Research 13 (3), 216-225.

[23] Kokjohn S L, Hanson R M, Splitter D A, Reitz R D. Fuel reactivity controlled compression ignition (RCCI): a pathway to controlled high-efficiency clean combustion, International Journal of Engine Research, 2011. Volume 12, June 2011, Pages 209-226.

[24] Benajes J, Molina S, García A, Monsalve-Serrano J. Effects of low reactivity fuel characteristics and blending ratio on low load RCCI (reactivity controlled compression ignition) performance and emissions in a heavy-duty diesel engine. Energy, Volume 90, October 2015, Pages 1261–1271.

[25] Benajes J, Molina S, García A, Monsalve-Serrano J. Effects of Direct injection timing and Blending Ratio on RCCI combustion with different Low Reactivity Fuels. Energy Conversion and Management, Volume 99, July 2015, Pages 193-209.

[26] Benajes J, García A, Monsalve-Serrano J, Sari R. Experimental investigation on the efficiency of a diesel oxidation catalyst in a medium-duty multi-cylinder RCCI engine. Energy Conversion and Management, Volume 176, 15 November 2018, Pages 1-10

[27] García, A., Piqueras, P., Monsalve-Serrano, J., Lago Sari, R. Sizing a conventional diesel oxidation catalyst to be used for RCCI combustion under real driving conditions. Applied Thermal Engineering Volume 140, 2018, Pages 62-72

[28] Benajes J, García A, Monsalve-Serrano J, Villalta D. Exploring the limits of the RCCI combustion concept in a light-duty diesel engine and the influence of the direct-injected fuel properties. Energy Conversion and Management, Volume 157, 2018, Pages 277-287.

[29] Benajes J, García A, Monsalve-Serrano J, Balloul I, Pradel G. Evaluating the reactivity controlled compression ignition operating range limits in a high-compression ratio medium-duty diesel engine fueled with biodiesel and ethanol. International Journal of Engine Research, Volume 18 (1-2), Pages 66-80, 2017.

[30] Molina S., García A., Monsalve-Serrano J., Estepa D. Miller cycle for improved efficiency, load range and emissions in a heavy-duty engine running under reactivity controlled compression ignition combustion. Applied Thermal Engineering, Volume 136, 2018, Pages 161-168.

[31] Pedrozo V., May W., Guan W., Zhao H. High efficiency ethanol-diesel dual-fuel combustion: A comparison against conventional diesel combustion from low to full engine load. Fuel, Volume 230, 2018, Pages 440-451, ISSN 0016-2361, https://doi.org/10.1016/j.fuel.2018.05.034.

[32] Benajes J, García A, Monsalve-Serrano J, Boronat V. Achieving clean and efficient engine operation up to full load by combining optimized RCCI and dual-fuel diesel-gasoline combustion strategies. Energy Conversion and Management, Volume 136, 15 March 2017, Pages 142-151.

[33] García A, Monsalve-Serrano J, Rückert Roso V, Santos Martins M. Evaluating the emissions and performance of two dual-mode RCCI combustion strategies under the World Harmonized Vehicle Cycle (WHVC). Energy Conversion and Management, Volume 149, 1 Oct 2017, Pages 263-274.

[34] Benajes, J., García, A., Pastor, J.M., Monsalve-Serrano, J. Effects of piston bowl geometry on Reactivity Controlled Compression Ignition heat transfer and combustion losses at different engine loads. Energy, Volume 98, March 2016, pages 64-77.

[35] AVL manufacturer manual. Smoke value measurement with the filter-papermethod. Application notes. June 2005 AT1007E, Rev. 02. Web:<https://www.avl.com/documents/10138/885893/Application+Notes >.

[36] Luján, J. M., Dolz, V., Monsalve-Serrano, J., & Bernal Maldonado, M. A. (2019). High-pressure exhaust gas recirculation line condensation model of an internal combustion diesel engine operating at cold conditions. International Journal of Engine Research. https://doi.org/10.1177/1468087419868026

[37] Payri R., Gimeno J., Mata C., Viera A. Rate of injection measurements of a direct-acting piezoelectric injector for different operating temperatures. Energy Conversion and Management, Volume 154, 2017, Pages 387-393, ISSN 0196-8904, https://doi.org/10.1016/j.enconman.2017.11.029.

[38] Vinícius B. Pedrozo, Ian May, Hua Zhao. Exploring the mid-load potential of ethanol-diesel dual-fuel combustion with and without EGR. Applied Energy, Volume 193, 2017, Pages 263-275.

Abbreviations

ATDC: After Top Dead Center

$BSFC_{eq}$: Equivalent Brake Specific Fuel Consumption

CAD: Crank Angle Degree

CDC: Conventional Diesel Combustion

CO: Carbon Monoxide

CO_2: Carbon Dioxide

COP 21: Conference Of Parties 21^{st} edition

COV: Coefficient of Variation

DI: Direct Injection

DMDF: Dual Mode Dual Fuel

EGR: Exhaust Gas Recirculation

FIS: Fuel Injection System

FSN: Filter Smoke Number

HC: Hydro Carbons

HRR: Heat Release Rate

HRF: High Reactivity Fuel

IMEP: Indicated Mean Effective Pressure

LRF: Low Reactivity Fuel

LTC: Low Temperature Combustion

LTHR: Low Temperature Heat Release

LHV: Lower Heating Value

NOx: Nitrogen Oxides

OMEx: Oxymethylene Ether

PER: Premix Energy Ratio

PFI: Port Fuel Injection

RCCI: Reactivity Controlled Compression Ignition
RON: Research Octane Number
SOI: Start of Injection
TDC: Top Dead Center
MON: Motor Octane Number
VGT: Variable Geometry Turbine
WHVC: Worldwide Harmonized Vehicle Cycle